Giant Tumefactive Perivascular Spaces

Karen L. Salzman, Anne G. Osborn, Paul House, J. Randy Jinkins, Adam Ditchfield,
James A. Cooper, and Roy O. Weller

BACKGROUND AND PURPOSE: **The brain perivascular spaces (PVSs) are pial-lined, interstitial fluid-filled structures that accompany penetrating arteries. When enlarged, they may cause mass effect and can be mistaken for more ominous pathologic processes. The purpose of this study was to delineate the broad clinical and imaging spectrum of this unusual condition.**

METHODS: **Thirty-seven cases of giant PVSs were identified from 1988 to 2004 and were retrospectively reviewed. Clinical data collected included patient demographics, presenting symptoms, and follow-up. Histopathologic data were reviewed when available. Images were evaluated for size and location of the giant PVSs, associated mass effect, hydrocephalus, adjacent white matter changes, and contrast enhancement.**

RESULTS: **There were 24 men and 13 women with an age range of 6–86 years, (mean 46 years). The most common presenting feature was headache (15 patients). Thirty-two cases had multilocular clusters of variably sized cysts. Five lesions were unilocular. All lesions had signal intensity comparable to CSF and did not enhance. The most common location for the giant PVSs was the mesencephalothalamic region (21/36). Fourteen were located in the cerebral white matter; two were in the dentate nuclei. Nine giant mesencephalothalamic PVSs had associated hydrocephalus, which required surgical intervention.**

CONCLUSION: **Giant tumefactive PVSs most often appear as clusters of variably sized cysts that are isointense relative to CSF and do not enhance. They are most common in the mesencephalothalamic region and may cause hydrocephalus. Although they may have striking mass effect, giant PVSs should not be mistaken for neoplasm or other diseases.**

The perivascular spaces (PVSs) of the brain, also known as Virchow-Robin spaces, are pial-lined interstitial fluid (ISF)-filled structures that accompany penetrating arteries and arterioles for a variable distance as they descend into the cerebral substance (1–3). Recent studies have shown that the PVSs are surprisingly complex entities with significant variability in both ultrastructure and possible function. Routinely, PVSs in many areas of the brain can be identified on MR images obtained in patients of all ages

(4). Occasionally the PVSs may become strikingly enlarged, causing mass effect and assuming bizarre configurations that may be mistaken for a more ominous disease, such as a cystic neoplasm (Figure 1). While scattered cases of giant tumefactive PVSs have been reported (5–7), no large series of these lesions has been presented. The purpose of this study is to delineate the broad clinical and imaging spectrum of giant tumefactive perivascular spaces to further characterize this unusual lesion.

Methods

We performed a retrospective review of all cases of giant PVSs referred for imaging consultation or treated at our institution over a 16-year period spanning 1988 to 2004. Most cases referred for second opinion had the presumptive diagnosis of cystic neoplasm.

We defined giant PVSs as equal to or greater than 1.5 cm, occurring as either a solitary lesion or in clusters of multiple contiguous cysts.

Clinical data collected included patient age, sex, and presenting symptoms. Histopathologic data in patients who underwent biopsy were collected and reviewed. The specific histologic stains used included: Hematoxylin and Eosin as a general histologic stain; Hematoxylin van Gieson to stain the collagen of the meninges on the outer aspect of the cyst wall; and reticulin to stain the collagen of the meninges on the outer aspect of the cyst wall.
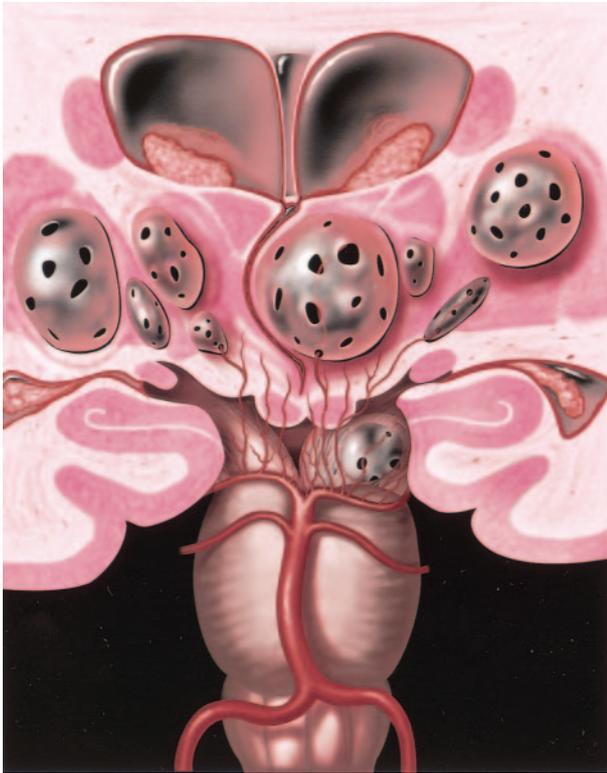
FIG 1. Coronal anatomic diagram depicts multiple bilateral giant perivascular spaces (PVSs) in the mesencephalothalamic region. There are fenestrations of the giant PVSs, which may allow accumulation of interstitial fluid between the vessel and pia or within the interpial space causing enlargement of the PVSs. Note the mass effect upon the third ventricle with associated obstructive hydrocephalus. Graphic courtesy of James Cooper, MD and AMIRSYS, Inc (35).

All patients were imaged with MR imaging using a variety of 1.5T MR imaging units. Typical pulse sequences included T1-weighted spin-echo images, fast spin-echo T2-weighted images, proton density–weighted (PD) images, and fluid attenuated inversion recovery (FLAIR) images. Patients' MR imaging examinations included either a PD or FLAIR sequence. Gadolinium-enhanced T1-weighted imaging was also performed in most patients (34/36). Two studies were performed without the use of contrast medium. Ten patients underwent CT performed with 5-mm axial sections.

Images were evaluated to determine the size of the giant PVSs, establish whether cysts were unilateral or bilateral, and ascertain whether cysts were solitary or clustered. Images were also assessed for the appearance of associated focal or generalized mass effect, hydrocephalus, adjacent white matter changes, and presence of contrast enhancement.

Results

Demographics

Thirty-seven patients with giant PVSs were identified, including 24 men and 13 women (M:F = 1.8:1). Patient age ranged from 6 to 86 years with a mean of 46 years. Five unilocular lesions were identified ranging in size from 1.5 cm to 3.5 cm. Multiple clustered cysts (32/37 cases) were present in most cases. The clusters were all greater than or equal to 1.5 cm in size, ranging from 1.5 cm to 10 cm in greatest dimen-

TABLE 1: Presenting symptoms

Headache	15
Dizziness	3
Dementia	3
Visual changes	3
Post-traumatic evaluation	2
Cranial neuropathy	2
Seizure	1
Syncope	1
Stroke	1
Memory problems	1
Poor balance and concentration	1
N = 33	

sion. There were 27 unilateral lesions and 10 bilateral lesions.

Clinical Findings:

Complete clinical data were available in 33 patients with a partial history available in the remaining four patients. The most common presenting symptom was headache, present in 15/33 patients. Other presenting features included dizziness, dementia, visual changes, post-traumatic evaluation, seizure, syncope, stroke, memory problems, cranial neuropathy and poor balance and concentration. One additional patient had a 6th nerve palsy which was found to be related to diabetic neuropathy and resolved on follow-up imaging. One patient who presented with visual changes was ultimately diagnosed with uveitis, which was treated and resolved (Table 1).

Imaging Findings

CT was performed in 10 of 37 patients. All giant PVSs were low-attenuation lesions, isoattenuated relative to CSF, which showed no enhancement following contrast medium administration. No calcifications or other associated abnormalities were identified.

All giant PVSs were isointense relative to CSF signal intensity on all MR images regardless of pulse sequence. Contrast-enhanced images were available in 35/37 cases and showed no enhancement. Diffusion-weighted (DW) imaging was available in eight of 37 cases and showed no diffusion restriction.

Lesions were subdivided by location (Table 2). There were 21 patients with lesions involving the midbrain or thalamus (mesencephalothalamic area) (Fig 2) and 14 lesions predominately involved the hemispheric or subcortical cerebral white matter. Two lesions were present in the region of the dentate nuclei of the cerebellar hemispheres.

Of the 21 mesencephalothalamic lesions, four were bilateral. No signal intensity alteration was present in the adjacent brain parenchyma. Nine of these 21 mesencephalothalamic lesions had associated hydrocephalus and were treated with ventriculostomy (5), ventriculoperitoneal shunting (3), or cystoperitoneal shunting (1) (Fig 3).

There were 14 patients with giant PVSs in the cerebral white matter (Fig 4). Five of these white

TABLE 2: Lesion location and follow-up

Age	Sex	Giant PVS Location	Biopsy	Follow-up Imaging
39	M	Thalamus	Y	2 years
76	M	Thalamus	N	N
56	F	Thalamus	N	4 years
86	M	Thalamus	N	12 years
35	M	Thalamus	N	2 years
42	F	Thalamus	N	N
49	F	Thalamus	N	7 years
35	M	Midbrain	Y	1 year
57	M	Midbrain	Y	N
44	F	Midbrain	N	N
75	M	Midbrain	N	N
40	M	Midbrain	Y	N
28	M	Midbrain	N	N
35	M	Midbrain/Pons	Y	1 year
47	F	Thalamus/Midbrain	N	9 years
62	M	Thalamus/Midbrain	N	N
46	M	Thalamus/Midbrain	Y	N
75	M	Thalamus/Midbrain	N	1 year
72	F	Thalamus/Basal Ganglia	N	10 years
41	M	Basal Ganglia	N	1 year
47	M	Basal Ganglia	N	N
15	M	White Matter	N	7 years
70	M	White Matter	N	N
62	F	White Matter	N	N
37	M	White Matter	N	1 year
68	M	White Matter	N	N
56	F	White Matter	N	N
44	F	White Matter	N	1 year
21	M	White Matter	Y	6 years
36	M	White Matter	N	2 years
68	F	White Matter	N	N
46	F	White Matter	N	N
20	F	White Matter	N	N
40	F	White Matter	N	N
10	M	White Matter	N	3 years
17	M	Cerebellum	N	N
6	M	Cerebellum	N	N

matter cases were bilateral. White matter lesions were located in the subcortical white matter (8/14), hemispheric white matter (4/14), or both (2/14). Most white matter lesions involved the frontal lobe (8/14) with other areas of involvement including the parietal lobe (3/14), temporal lobe (2/14), and occipital lobe (1/14). There was involvement of the cingulate gyrus subcortical white matter in four cases and three cases had involvement of the corpus callosum. In these cases, the gray matter was stretched over the giant PVSs (Fig 5).

Associated white matter signal intensity alterations occurred in seven of the cerebral white matter cases. Two of these were focal changes, with increased T2 and FLAIR signal intensity, surrounding the giant PVSs, and were found in older patients (a 68-year-old woman and a 73-year-old man) (Fig 4). Five additional patients with lesions in the white matter had more diffuse, confluent abnormal signal intensity alteration consisting of increased T2 and FLAIR signal intensity surrounding the PVSs (Fig 6).

There were two lesions that involved the region of the cerebellar dentate nuclei. In one case, the lesions were bilateral. There was no associated signal intensity alteration in the adjacent brain parenchyma (Fig 7).

Surgical and Pathologic Findings

Surgery was performed in 12 patients. In seven cases, biopsy was performed. Histopathologic results in most cases (6/7) disclosed a pial-lined cyst with no evidence of neoplasm or infection. One patient with a midbrain lesion had a layer of pia and arachnoid on the outer aspect of the tissue but no pial lining. This patient had a small fragment, approximately 1 mm cubed, of the cyst lining sent to the pathology department. It was fixed in formalin, embedded in paraffin, and stained with hematoxylin and eosin, hematoxylin van Gieson for collagen, and by immunocytochemistry for glial fibrillary acidic protein (GFAP) for astrocytes Figure 8. Figure 8A shows the cyst lining consists of a very thin layer of gliotic brain tissue coated on its outer aspects by collagenous material related to the pia arachnoid on the surface of the midbrain. No lining of pia matter was identified on the inner cyst surface. The brain tissue lining the cyst was extensively gliotic as shown in the GFAP preparation (Fig 8B). Close examination of the cells in the brain tissue lining the cyst shows that it is mainly composed of astrocytes (Fig 8C). The absence of a lining of pia matter is only to be expected in this case, as the cyst was very large and it is unlikely that the thin delicate lining surrounding a vessel would be stretched to this extent. When there is less extensive enlargement of perivascular spaces, the lining of pia matter may remain.

Two patients had a ventriculoperitoneal shunt placed, and the size of the giant PVSs was stable in each case. Another patient had a cystoperitoneal shunt placed, and there was a decrease in the size of the giant PVS from 10 cm to 5 cm. In this case, the patient's headache also improved. However, the fluid reaccumulated after the patient had a minor traumatic insult, and the giant PVS enlarged to near-presentation size. One patient underwent PVS drainage followed by ventriculoperitoneal shunt placement after the PVS returned to its original size. Five patients underwent a third ventriculostomy; three of these patients also had a biopsy of the cyst wall.

Follow-up MR imaging was available in seventeen patients from 1–12 years after the initial diagnosis. No interim change was seen on repeat MR imaging in any case.

Discussion

When PVSs become markedly expanded, they can be misinterpreted as other pathologic processes, most often a cystic neoplasm. As most of these cysts border a ventricle or subarachnoid space, reports of such cases have offered an extensive differential diagnosis that includes cystic neoplasms, parasitic cysts, ventricular diverticula, cystic infarction, non-neoplastic neuroepithelial cysts, and deposition disorders such as mucopolysaccharidosis (4, 7–9). The aim of this study
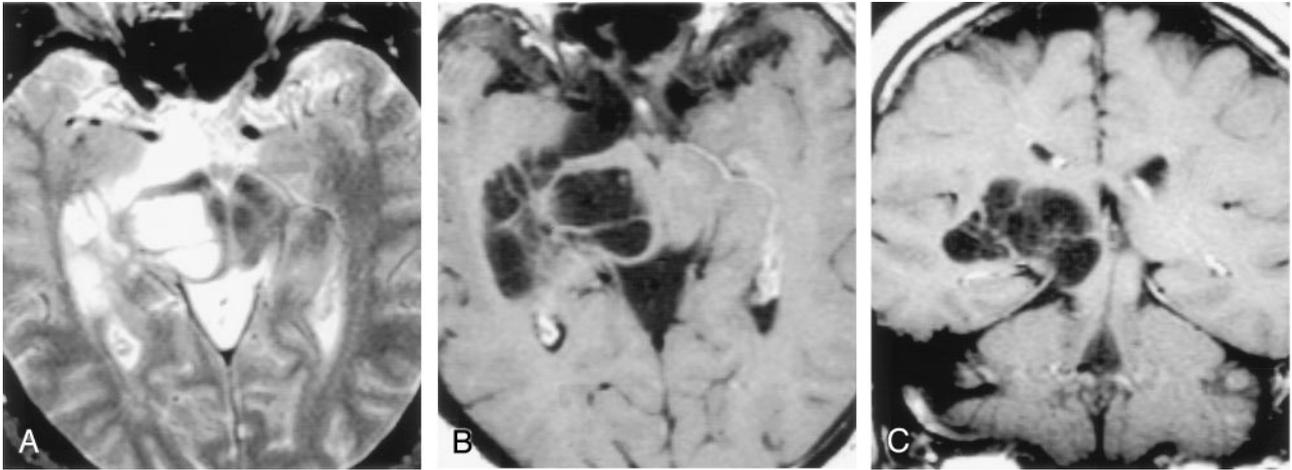
FIG 2. Axial T2-weighted (A), postcontrast axial T1-weighted (B), and postcontrast coronal T1-weighted (C) images obtained in a 46-year-old man with headaches show a nonenhancing multiloculated cystic mass in the right midbrain, thalamus, and right medial temporal lobe. The cysts follow CSF signal intensity on all pulse sequences and do not enhance. Follow-up imaging 13 years later showed no change. Biopsy proved pial-lined giant perivascular spaces.
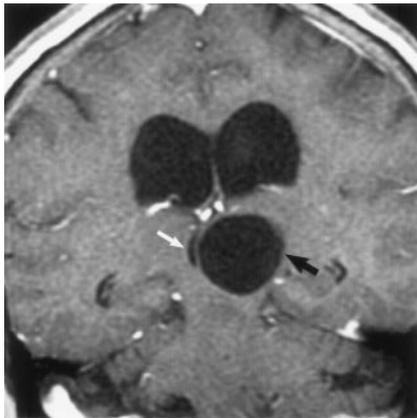

FIG 3. Coronal postcontrast T1-weighted image obtained in a 56-year-old woman with headaches shows a nonenhancing unilocular giant perivascular space (black arrow) in the left thalamus with compression and displacement of the third ventricle (white arrow). Note associated hydrocephalus. Surgery disclosed a smooth walled cyst with no abnormality in the adjacent brain. The patient initially underwent a cyst fenestration with a decrease in the size of the PVS. Four months later, there was reaccumulation of fluid and the PVS enlarged to its original size. A ventriculoperitoneal shunt was then placed, which relieved the hydrocephalus. Follow-up studies showed no change in cyst size over 4 years.

was to delineate the classic imaging appearance of giant PVSs in an effort to prevent misdiagnosis and unnecessary biopsy.

Typical PVSs occur in many locations. The most common site is along the lenticulostriate arteries, just above the anterior perforated substance and adjacent to the anterior commissure. Less commonly, PVSs occur along arteries that have penetrated the cerebral cortex and extended into the white matter (4, 8). Other areas where prominent PVSs can be identified include the subinsular region, dentate nuclei, and cerebellum (2). PVSs have typical MR imaging features as previously described. They are round or oval with a well-defined, smooth margin, occur along the path of penetrating arteries, are isointense relative to

CSF, and demonstrate no enhancement following contrast medium administration (4, 6, 8, 9). When PVSs become enlarged, they are known as giant PVSs, "cavernous dilatation," or Poirier's Type IIIb "expanding lacunae" (6, 10, 11).

Giant PVSs are expanded PVSs that occur along the penetrating vessels, most commonly in the mesencephalothalamic region in the territory of the paramedial mesencephalothalamic artery and in the cerebral white matter (4, 7, 10). They differ from typical PVSs in that they are larger in size and may have associated focal mass effect. In addition, white matter giant PVSs may have associated T2 and FLAIR signal intensity alteration in the adjacent white matter.

Patients usually present with nonspecific findings that are not attributable to the giant PVSs. In our series, headache was the most common presenting feature and occurred in approximately 50% of our patients. Other presenting complaints included dizziness, dementia, visual changes, post-trauma, seizure, syncope, memory problems, poor balance, and poor concentration. Several studies have found that the clinical features of patients with this type of lesion do not correlate with the imaging findings or have been found incidentally at autopsy (9,12–14). However, widespread dilatation of the PVSs has been reported in association with dementia and parkinsonism (15, 16). Some authors have correlated large convexity and white matter PVSs with increasing age (4). Others have concluded that the prevalence of basal ganglia PVSs in patients younger than 40 years is not significantly different from that of older patients (8). We have observed prominent PVSs on high-spatial-resolution MR images in patients of all ages and in all typical anatomical locations. The clinical symptoms did not correlate with the giant PVSs in our series, except in those cases that had associated hydrocephalus, requiring CSF diversion.

Imaging of enlarged PVSs is characteristic (17, 18). All cases have associated mass effect, from mild to severe. The mass effect may occasionally cause ob-
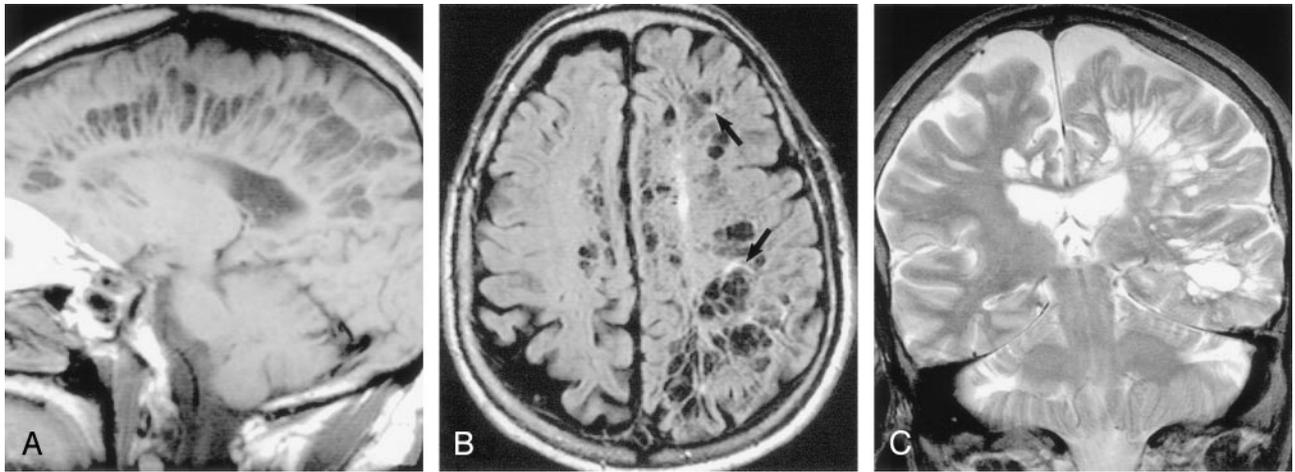
FIG 4.   Sagittal T1-weighted (A), axial FLAIR (B), and coronal T2-weighted (C) images obtained in a 71-year-old man with dementia show extensive involvement of the hemispheric and subcortical white matter with multilocular giant perivascular spaces. The coronal image shows the marked asymmetry of the lesions. Note the scattered focal white matter changes surrounding some of the lesions (black arrows) seen best on the FLAIR image. Case courtesy of Anthony Doyle, MD.
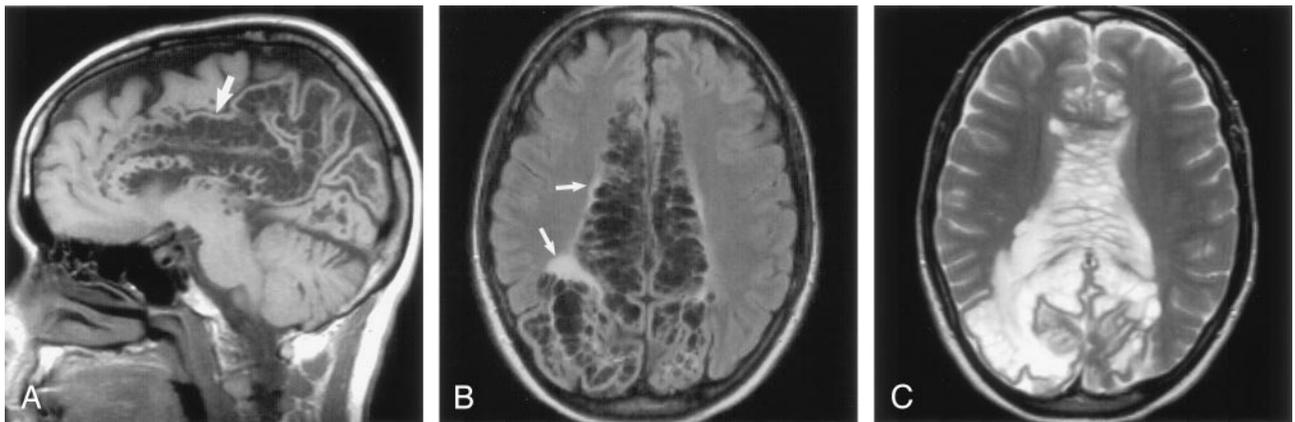

FIG 5.   Sagittal T1-weighted (A), axial FLAIR (B), and axial T2-weighted (C) images obtained in a 46-year-old woman with a visual field defect show extensive involvement of the corpus callosum and cingulate gyrus (A, white arrow) with extension to the subcortical white matter of the parietal and occipital lobes. There is slight increased signal intensity surrounding the lesions, best seen on FLAIR image (B, white arrows). The gray matter is stretched and displaced over the multiloculated giant perivascular spaces. Case courtesy of Leena Valanne, MD.
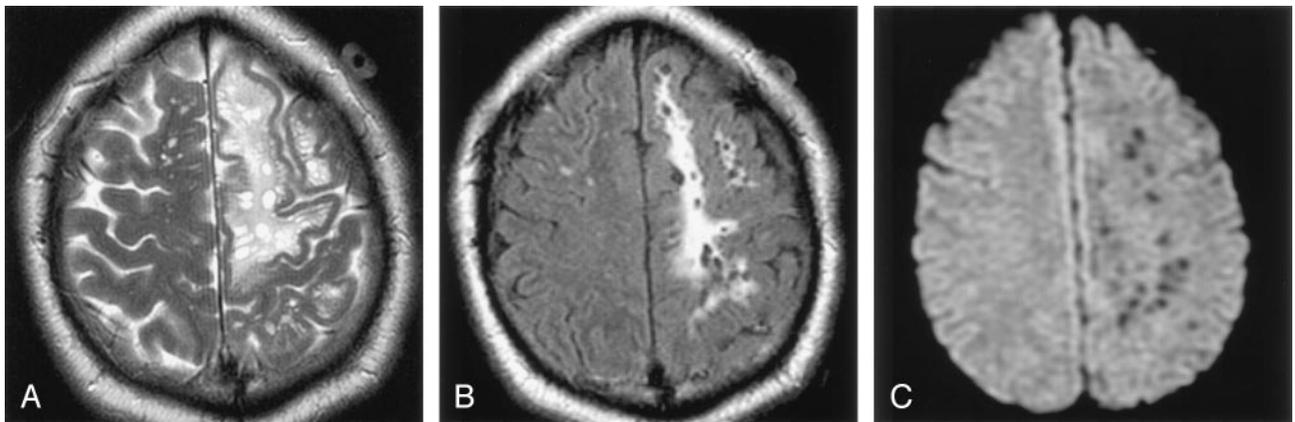

FIG 6.   Images obtained in a 37-year-old man with headaches. Axial T2-weighted (A) and axial FLAIR (B) images show diffuse, confluent white matter hyperintensity surrounding the giant perivascular spaces. There is mild gyral expansion over the perivascular spaces. The diffusion-weighted image (C) shows no diffusion restriction.

structive hydrocephalus as was seen in eight of our study patients, all with lesions in the mesencephalo-

thalamic region. Associated hydrocephalus has been reported in the literature and may require surgical
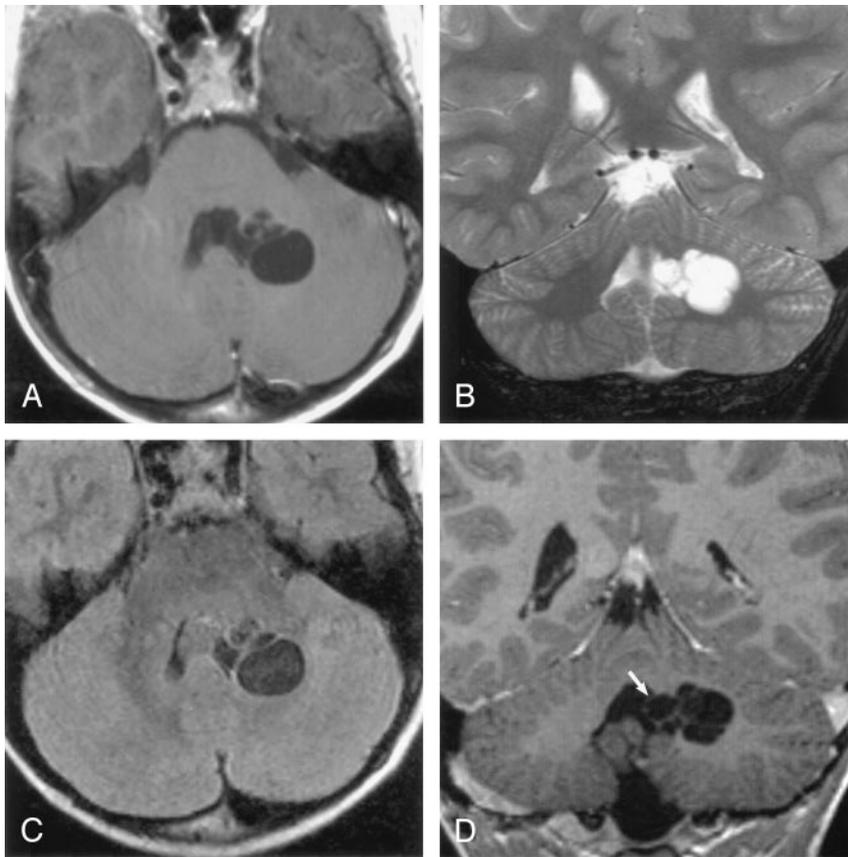
FIG 7. Images obtained in a 6-year-old boy with a history of minor trauma. Axial T1-weighted (A), coronal T2-weighted (B), axial FLAIR (C) and postcontrast coronal T1-weighted (D) images show multiloculated giant perivascular spaces in the left dentate gyrus. There is mild focal mass effect upon the fourth ventricle (white arrow). The clustered cysts follow CSF on all pulse sequences.

shunt surgery (19). FLAIR imaging typically shows complete signal intensity suppression without abnormalities in the adjacent parenchyma. In a few reported cases, small foci of high signal intensity adjacent to the cystic spaces have been identified (20). Our study shows that giant PVSs that occur in the white matter may have surrounding signal intensity abnormality seen on T2-weighted or FLAIR images, as seen in half of our cases. Lesions with adjacent white matter changes can be divided into two groups. In elderly patients in our series, the white matter changes surrounding the dilated PVSs were discrete areas of abnormal T2 and FLAIR hyperintense signal intensity abnormality. One possible theory is that this associated signal intensity alteration may represent advanced chronic ischemic change related to mass effect of the PVSs (5). Another possibility is that dilated PVSs may result from chronic mechanical stress caused by high blood pressure on the brain arterioles (21). However, most hypertensive patients imaged do not have associated giant PVSs.

In younger patients in our series, the signal intensity abnormality was more diffuse, with confluent T2 and FLAIR increased signal intensity surrounding the giant PVSs. Although the exact etiology is not known, we suggest that the changes may be secondary to gliosis or spongiosis. Alternatively, the signal intensity changes may be related to multiple tiny tightly clustered PVSs that are too small to be discriminated on the basis of current MR imaging findings. Abnormal hyperintensity in the cerebral white matter on T2-weighted images occurs in more than 30% of the neurologically healthy elderly population (9, 22, 23). Histopathologic study with MR imaging correlation has indicated that many of these lesions are PVSs (8, 24–26). One author found that PVSs greater than 2 mm were found in 67 (8%) of 816 patients (4).

Giant PVSs (up to 2–3 cm in diameter) have been reported to occur as a normal variant (4, 27). The precise etiology of these enlarged PVSs is unknown. Spiral elongation of the penetrating blood vessels has been suggested as one possible cause of this phenomenon (24). Increased CSF pulsations, the *ex vacuo* phenomenon, or an abnormality of arterial wall permeability have also been cited as contributing factors (9, 13, 28, 29).

Experimental studies suggest that the periarterial spaces are the routes by which interstitial fluid (ISF) drains from brain tissue (30). In humans, amyloid–beta (Aβ) appears to be entrapped within the drainage pathways in the cerebral amyloid angiopathy that accompanies Alzheimer disease (AD) (31, 32). Although the periarterial spaces in the cortex are not dilated in AD, periarterial spaces in the white matter are expanded possibly due to obstruction of ISF drainage pathways by Aβ in the proximal parts of each artery (33). By analogy, obstruction of ISF drainage pathways could be a major factor in the pathogenesis of giant PVSs, although the exact nature of the obstruction is unclear.

Other investigators have postulated that because the pial membrane surrounding the penetrating ar-
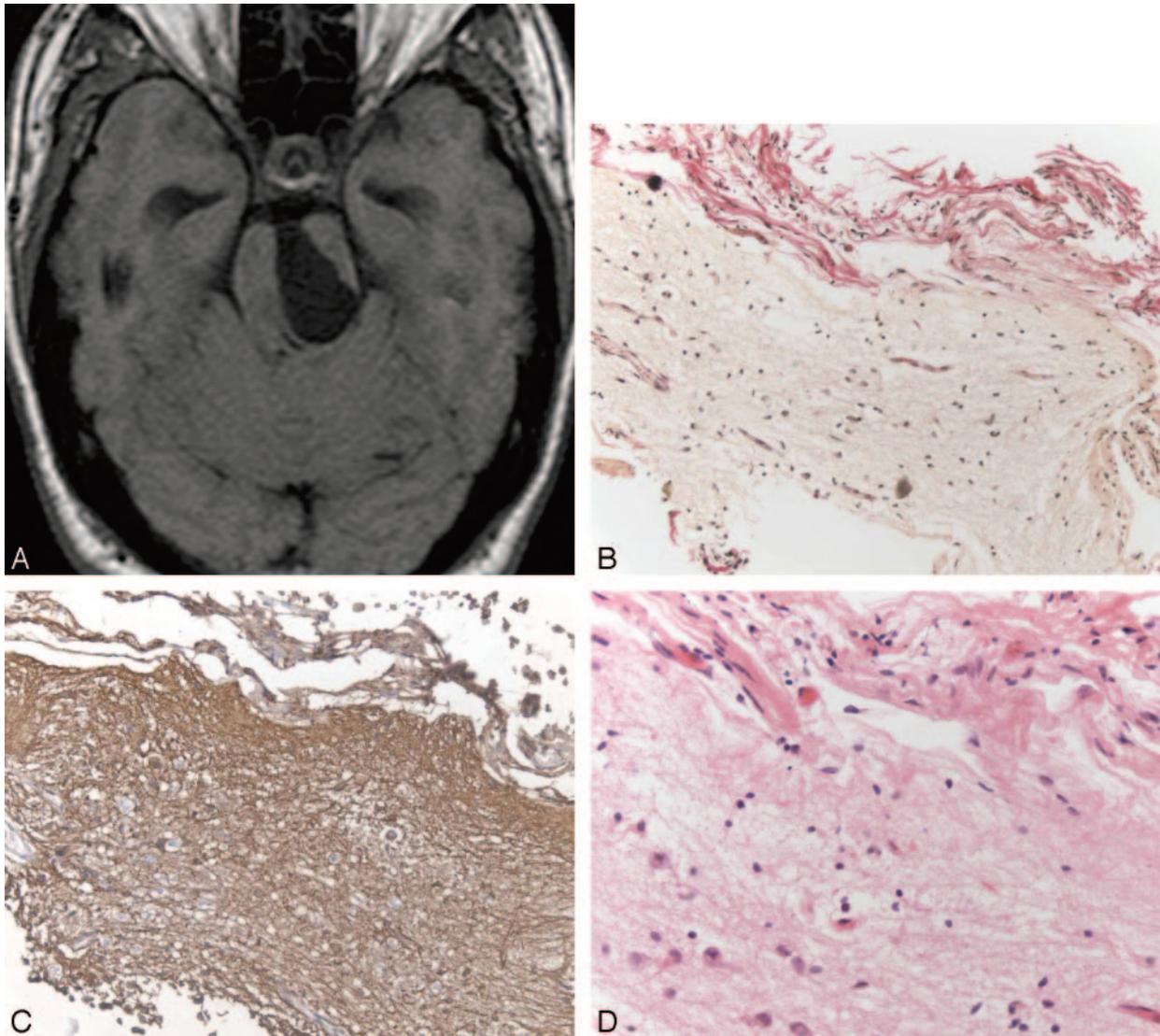
FIG 8.   Images obtained in a 35-year-old man with headache who underwent a biopsy and a third ventriculostomy procedure. Axial T1-weighted MR image (A) shows the giant perivascular space in the left midbrain. A section through the cyst wall (B) shows red-stained collagen in the leptomeninges on the outer aspect of the cyst wall coating the underlying brain tissue that forms the bulk of the cyst wall. No lining of pia matter is present on the inner aspect of the cyst. (Hematoxylin van Gieson stain, original magnification ×20) There is extensive gliosis in the cyst wall as demonstrated by the numerous brown stained fibrillary processes within the brain tissue (C). (Immunocytochemistry for GFAP, original magnification ×20) A high-power view (D) of the cyst wall near the pia arachnoid outer coating (top of picture). Reactive astrocytes are seen toward the bottom of the illustration. No neurons were identified. (Hematoxylin and eosin stain, original magnification ×40)

tery is fenestrated, accumulation of brain interstitial fluid between the vessel and pia or within the inter-pial space causes the PVSs to enlarge (27). We found that giant PVSs are most common in the mesen-cephalothalamic region, which may indeed be related to the two layers of pia in this location. In addition, the significant mass effect with associated obstructive hydrocephalus seen in the mesencephalothalamic group may, in part, be related to the two pial layers.

Giant PVSs with mass effect may occur as single or multiple clustered cysts that can be mistaken for more ominous disease (34). When the lesions in question occur in a characteristic location along the path of a penetrating vessel, follow CSF signal intensity on all sequences, do not enhance with contrast material, and have normal adjacent brain parenchyma, their appearance is virtually pathognomonic of giant PVSs. An extensive differential diagnosis is superfluous and biopsy unnecessary (14).

Conclusion

Giant tumefactive PVSs are interstitial-fluid filled structures that accompany arteries and arterioles as they penetrate the brain. They have characteristic imaging features: round or oval, single or multilocular lesions that are isointense relative to CSF regardless of imaging sequences and do not enhance. They are most common in the mesencephalothalamic region and may have associated obstructive hydrocephalus that may require surgical intervention. Although they

have associated mass effect, they should not be mistaken for neoplasm or other disease.

References

1. Ozturk MH, Aydingoz U. **Comparison of MR signal intensities of cerebral perivascular (Virchow-Robin) and subarachnoid spaces.** *J Comput Assist Tomogr* 2002;26:902–904
2. Song CJ, Kim JH, Kier EL, Bronen RA. **MR imaging and histologic features of subinsular bright spots on T2–weighted MR images: Virchow-Robin spaces of the extreme capsule and insular cortex.** *Radiology* 2000;214:671–677
3. Pollock H, Hutchings M, Weller RO, Zhang ET. **Perivascular spaces in the basal ganglia of the human brain: their relationship to lacunes.** *J Anat* 1997;191:337–346
4. Heier LA, Bauer CJ, Schwartz L, et al. **Large Virchow-Robin spaces: MR –clinical correlation.** *AJNR Am J Neuroradiol* 1989;10:929–936
5. Shiratori K, Mrowka M, Toussaint A, Spalke G, Bien S. **Extreme, unilateral widening of Virchow-Robin spaces: case report.** *Neuroradiology* 2002;44:990–992
6. Kanamalla US, Calabro F, Jinkins JR. **Cavernous dilatation of mesencephalic Virchow-Robin spaces with obstructive hydrocephalus.** *Neuroradiology* 2000;42:881–884
7. Homeyer P, Cornu P, Lacomblez L, et al. **A special form of cerebral lacunae: expanding lacunae.** *J Neurol Neurosurg Psychiatr* 1996;61:200–202
8. Jungreis CA, Kanal E, Hirsch WL, et al. **Normal perivascular spaces mimicking lacunar infarction: MR imaging.** *Radiology* 1988;169:101–102
9. Ogawa R, Okudera T, Fukasawa H, et al. **Unusual widening of Virchow-Robin spaces: MR appearance.** *AJNR Am J Neuroradiol* 1995;16:1238–1242
10. Poirier J, Barbizet J, Gaston A, Meyrignac C. **Thalamic dementia. Expansive lacunae of the thalamo-paramedian mesencephalic area. Hydrocephalus caused by stenosis of the aqueduct of Sylvius.** *Rev Neurol (Paris)* 1983;139:349–358
11. Poirier J, Gray F, Gherardi R, Derouesné C. **Cerebral lacunae. A new neuropathological classification.** *J Neuropathol Exp Neurol* 1985;44:312
12. Ugawa Y, Shirouzu I, Terao Y, et al. **Physiological analyses of a patient with extreme widening of Virchow-Robin spaces.** *J Neurol Sci* 1998;159:25–27
13. Benhaïem-Sigaux N, Gray F, Gherardi R, et al. **Expanding cerebellar lacunae due to dilatation of the perivascular space associated with Binswanger's subcortical arteriosclerotic encephalopathy.** *Stroke* 1987;18:1087–1092
14. Demaerel P, Wilms G, Baert AL. **Widening of Virchow-Robin spaces [letter].** *AJNR Am J Neuroradiol* 1996;17:800–801
15. Vital C, Julian J. **Widespread dilatation of perivascular spaces: A leukoencephalopathy causing dementia.** *Neuroradiology* 1997;48:1310–1313
16. Fénelon G, Gray F, Wallays C, et al. **Parkinsonism and dilatation of the perivascular spaces (état criblé) of the striatum: A clinical magnetic resonance imaging and pathological study.** *Movement Disorders* 1995;10:754–760
17. Yetkin FZ, Fischer ME, Papke RA, Haughton VM. **Focal hyperintensities in cerebral white matter on MR images of asymptomatic volunteers: correlation with social and medical histories.** *Am J Roentgenol* 1993;161:855–858
18. Bokura H, Kobayashi S, Yamaguchi S. **Distinguishing silent lacunar infarction from enlarged Virchow-Robin spaces: a magnetic resonance imaging and pathological study.** *J Neurol* 1998;245:116–22
19. Mascalchi M, Salvi F, Gordano U, et al. **Expanding lacunae causing triventricular hydrocephalus. Report of two cases.** *J Neurosurg* 1999;91:669–674
20. Komiyama M, Yasui T, Izumi T. **Magnet resonance imaging features of unusually dilated Virchow-Robin spaces—two case reports.** *Neurol Med Chir* 1998;38:161–164
21. Sawada M, Nishi S, Hashimoto N. **Unilateral appearance of markedly dilated Virchow-Robin spaces.** *Clin Radiol* 1999;54:334–336
22. Gerard G, Weisberg LA. **MRI periventricular lesions in adults.** *Neurology* 1986;36:998–1001
23. Drayer BP. **Imaging of the aging brain. Part I. Normal findings** *Radiology* 1988;166:785–796
24. Awad IA, Johnson PC, Spetzler RF, Hodak JA. **Incidental subcortical lesions identified on magnetic resonance imaging in the elderly II. Postmortem pathological correlations.** *Stroke* 1986;17:1090–1097
25. Elster AD, Richardson DN. **Focal high signal on MR scans of the midbrain caused by enlarged perivascular spaces: MR-pathologic correlation.** *AJR Am J Roentgenol* 1991;156:157–160
26. Braffman BH, Zimmerman RA, Trojanowski JQ, Gonatas NK, Hickey WF, Schlaepfer WW. **Brain MR: pathologic correlation with gross and histopathology. 1. Lacunar infarction and Virchow-Robin spaces.** *AJR Am J Roentgenol* 1988;151:551–558
27. Adachi M, Hosoya T, Haku T, Yamaguchi K. **Dilated Virchow-Robin spaces: MRI pathological study.** *Neuroradiology* 1998;40:27–31
28. Fazekas F, Kleinert R, Roob G, et al. **Histopathologic analysis of foci of signal loss on gradient-echo T2*-weighted MR images in patients with spontaneous intracerebral hemorrhage: Evidence of microangiopathy-related microbleeds.** *AJNR Am J Neuroradiol* 1999;20:637–642
29. Derouesné C, Gray F, Escourolle R, Castaigne P. **'Expanding cerebral lacunae' in a hypertensive patient with normal pressure hydrocephalus.** *Neuropath Appl Neurobiol* 1987; 13:309–320
30. Weller RO. **Pathology of cerebrospinal fluid and interstitial fluid of the CNS: significance for Alzheimer disease, prion disorders and multiple sclerosis.** *J Neuropathol Exp Neurol* 1998;57:885–894
31. Weller RO, Massey A, Newman TA, Hutchings M, Kuo YM, Roher AE. **Cerebral amyloid angiopathy: amyloid beta accumulates in putative interstitial fluid drainage pathways in Alzheimer's disease.** *Am J Pathol* 1998;153:725–733
32. Preston SD, Steart PV, Wilkinson A, Nicoll JAR, Weller RO. **Capillary and arterial cerebral amyloid angiopathy in Alzheimer's disease: defining the perivascular route for the elimination of amyloid beta from the human brain.** *Neuropathol Appl Neurobiol* 2003;29:106–117
33. Roher AE, Kuo YM, Esh C, et al. **Cortical and Leptomeningeal Cerebro-Vascular Amyloid and White Matter Pathology in Alzheimer's Disease.** *Molecular Medicine* 2003;9:112–122
34. Sato N, Sze G, Awad I, et al. **Parenchymal perianeurysmal cystic changes in the brain: Report of five cases.** *Radiology* 200;215:229–233
35. Osborn AG. **Brain Digital Teaching File.** Salt Lake City: Advanced Medical Imaging Reference Systems; 2003